Growth of a single-domain smectic phase in a thin liquid-crystalline polymer film

M. W. J. van der Wielen,[1] M. A. Cohen Stuart,[1] G. J. Fleer,[1] A. R. Schlatmann,[2] and D. K. G. de Boer[3]
[1]*Laboratory of Physical Chemistry and Colloid Science, Wageningen University, Dreijenplein 6, 6703 HB Wageningen, The Netherlands*
[2]*Philips CFT Materials Analysis Department, Professor Holstlaan 4, 5656 AA Eindhoven, The Netherlands*
[3]*Philips Research Laboratories, Professor Holstlaan 4, 5656 AA Eindhoven, The Netherlands*
(Received 22 April 1999)

The ordering process and kinetics in thin films (200–800-nm thick) of a thermotropic side-chain liquid-crystalline polymer have been investigated vertically and laterally, respectively, by x-ray reflectivity and atomic-force microscopy. The original smooth and amorphous spin-coated films initially become corrugated upon annealing in the smectic mesophase. The roughening of the surface results from the formation of randomly oriented microcrystalline domains in the film. At the same time, however, a laterally macroscopic crystal starts to grow from the substrate surface in the direction of the polymer-air interface at the expense of these domain structures. Finally, a nicely ordered single crystal with parallel-ordered bilayers is formed in the film as well as at the polymer-air interface. This one-dimensional crystallization, actually recrystallization, depends strongly on the temperature due to viscosity effects. At low temperatures, just above the glass-transition temperature, the ordering is very slow, but with increasing temperature the crystal growth is faster. An Arrhenius-type plot gives an activation energy of 122 kJ/mol, which we ascribe to the expected reorientations of the mesogenic groups during the recrystallization process. [S1063-651X(99)08209-4]

PACS number(s): 81.10.Aj, 61.10.Kw, 81.15.−z, 68.55.−a

I. INTRODUCTION

Liquid-crystalline materials represent an important field of study with many practical applications. Part of this field concerns liquid-crystalline polymers (LCPs). The study of thin films of such materials started about five years ago with the discovery that in thin films of thermotropic liquid-crystalline polymers (on a smooth substrate) perfect ordering can be achieved by a thermal treatment [1–4]. This kind of epitaxy results in a perfectly ordered one-dimensional single crystal. As a result of the ordering process, nanoscale surface structures appear. So far, the layering process (a kind of one-dimensional crystallization) and its kinetics have not been studied systematically.

In the case of classical polymers, crystallization can take place when their melts or solutions are cooled. Crystallization has also been investigated for thin films and close to interfaces [5,6]. One finding is that in thin films the crystal growth is definitely slower as compared to that in bulk due to the slowing down of the diffusion of molecules. Between the melting temperature and the glass-transition temperature the crystallization rate of polymers has a maximum. Starting from the melting point the rate of secondary nucleation increases as undercooling increases. However, at lower temperatures transport processes are slower due to the increasing viscosity, which will reduce the growth rate [7,8].

As for crystallization of classical polymers, the annealing temperature, the annealing time, and the film thickness of thin LCP films will play a crucial role in the ordering (crystallization) process. By changing these parameters it should be possible to influence the dynamics of ordering in and the final surface topography of thin liquid-crystalline polymer films and hence, to control the formation of (nanoscale) surface structures. Therefore, it is important to know how the crystallization process in thin LCP films takes place and on what time scale the ordering is completed.

The combination of x-ray reflectometry (XRR) and atomic-force microscopy (AFM) gives a good view on the morphology of and structures in the film and their changes in time. This motivates the present study.

II. EXPERIMENTAL SECTION

Films were prepared by spin coating from a 1,2-dichloroethane solution of the liquid-crystalline polymer LCP-C9 (depicted in Fig. 1) on silicon wafers (Wacker Chemitronics). Film thicknesses of about 200 and 800 nm were prepared. For the synthesis of the polymer, the cleaning of the substrates, and the spin-coating conditions, we refer to previous works [9–11]. The main step in the cleaning procedure is a plasma treatment.

The polymer used has a degree of polymerization of around 10 and has a glass-transition temperature, T_g, of 99 °C. Above this temperature two interdigitated smectic phases appear: a smectic *B* phase above 99 °C and a smectic *Ad* phase above 112 °C. The isotropization (melting) temperature (T_i) is at 165 °C. Full details about the synthesis and bulk characterization can be found elsewhere [10,11].

The samples were annealed on a hot stage at different temperatures for varying time intervals. Because of the finite time needed to heat up the sample (a few seconds) an uncertainty is present in the annealing time and temperature. To

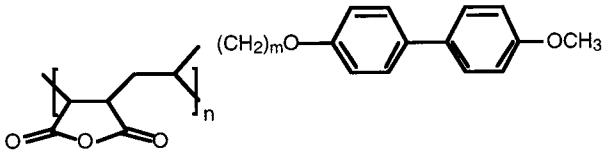

FIG. 1. Molecular structure of the repeating unit of the side-chain liquid-crystalline polymer, LCP-C9. The polymer studied has $m=9$, $n=10$, $T_g=99$ °C, $T_{s^B\rightarrow S^{Ad}}=112$ °C, and $T_{S^{Ad}\rightarrow I}=164$ °C.

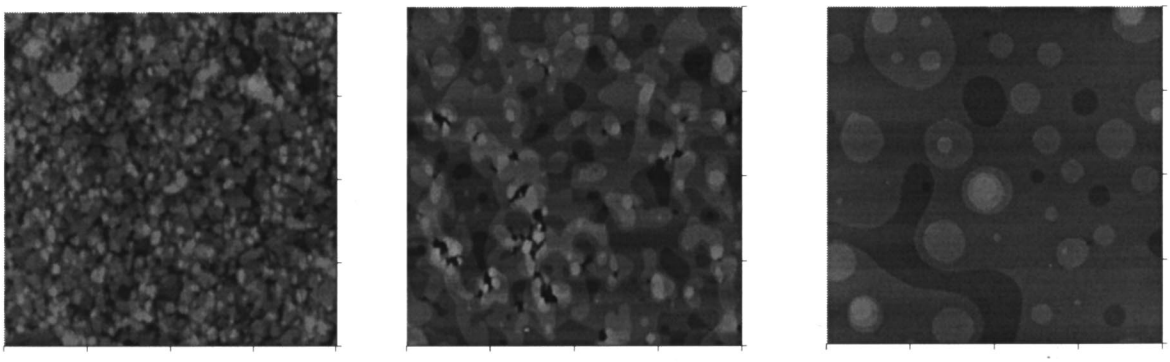

FIG. 2. AFM images of 10×10 μm^2) of a 210-nm thick film, annealed at 140 °C for 30 s (a), 1.5 min (b), and for 20 min (c) (black-white contrast in all images 40 nm).

minimize the relative uncertainty as much as possible all samples were annealed for at least 20 s, after which they were immediately cooled down on a cold red copper plate (stored in a refrigerator at -6 °C). In this way the temperature of the film is dropped rapidly to below T_g and the structure within the film is quenched.

In between the heating steps the films were analyzed at room temperature using an x-ray reflectometer (X'pert, Philips, SR5082) with a copper-anode tube. Symmetrical θ–2θ scans were performed with an incidence angle below 1.75° and the specular reflection was measured. A germanium 4-crystal monochromator (Ge220AS) with a divergence of 0.0042° was used for the incident beam, and the reflected beam is measured using a gas-filled detector with a 0.1-mm slit. The wavelength of the Cu $K\alpha$ beam is 0.154 nm. Analysis of the reflectivity data, resulting in electron-density profiles, thicknesses, and interfacial roughnesses, requires model assumptions. In model-fit calculations (program PHILIPS WINGIXA V1.1) the reflectivity is calculated and compared with the experimental data. Details about this program and the underlying method have been described by De Boer and co-workers [12,13].

The surface topography was investigated by AFM (Nanoscope III, Digital Instruments, Santa Barbara, CA) at room temperature, both for the as-prepared films and after annealing, in both contact mode (silicon-nitride cantilevers, spring constant about 0.58 N/m) as well as tapping mode (silicon cantilevers, spring constant between 25 and 110 N/m, and drive frequency of about 370 kHz).

III. RESULTS AND DISCUSSION

A. Crystallization processes

The investigated films (thickness 200 and 800 nm) are initially amorphous after spin coating (at room temperature) and have a smooth surface (roughness less than 1 nm, as determined by XRR and AFM. Upon annealing the films for several seconds in the mesophasic temperature range the polymer surface begins to roughen. Irregular structures are formed, the size of which increases with the film thickness. As an example, we show in Fig. 2(a) the surface topography (AFM image) of a film of 210-nm thickness annealed at 140 °C for 30 s. In Fig. 2(a) the width and height of the corrugations are typically about 500 and 25 nm, respectively. Under an optical microscope with crossed polarizers one also sees these small structures in the film.

After prolonged annealing (a few minutes) the domains, which were initially visible under crossed polarizers, disappear. However, the film does *not* become smooth. Under the AFM, a complicated structure with multiple terraces is found. This is shown in Fig. 2(b), which has been taken after a total annealing time at 140 °C of 1.5 min. It can be seen that the terraces are bounded by a smooth circumference. The typical lateral size of the ''hills'' is now about 1 μm. Further annealing (total annealing time 20 min) results in the growth of the terraces together with a reduction in their number, as shown in Fig. 2(c). For this growth to occur molecules have to be transported within the bilayers, as well as cross over from one bilayer into a neighboring one. Ausserré *et al.* [14] have modeled this process of permeation and interlayer transport of molecules.

A very striking ''landscape'' is given in Fig. 3 for a film of about a 800-nm thickness, which was annealed at 145 °C for 10 min. Up to 20 terrace levels can be seen. The step height between terraces (3.2 nm) corresponds precisely to the spacing of one interdigitated bilayer [4] The lateral size of the terraces is of the order of microns. When we compare Figs. 2(b) and 2(c) with Fig. 3, it seems that the thickness of the original film has an influence on the final size of the terraced ''hills.'' It is striking that the terraces are all perfectly parallel to the substrate. We note that the terraces have

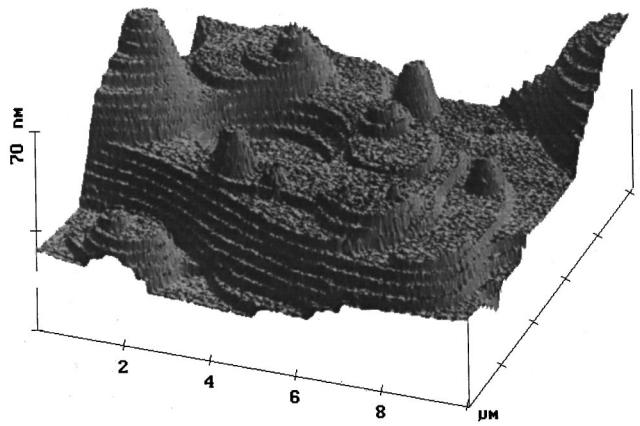

FIG. 3. AFM image (10×10 μm^2) of a 800-nm thick film, annealed at 145 °C for 10 min.

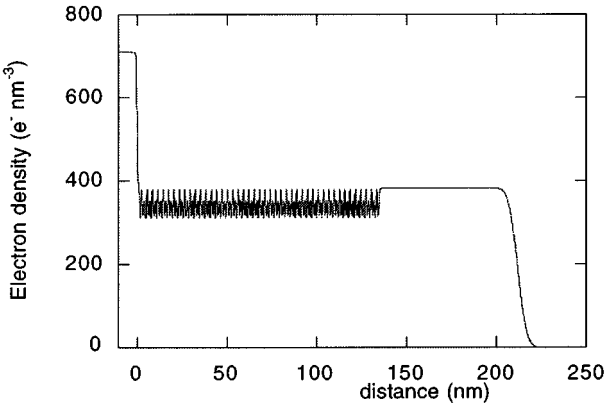

FIG. 4. Electron-density profile (from x-ray reflectivity) for a 210-nm thick film, annealed at 140 °C for 20 s. At the left side the silicon substrate is located with a density of approximately 700 $e\ \mathrm{nm}^{-3}$.

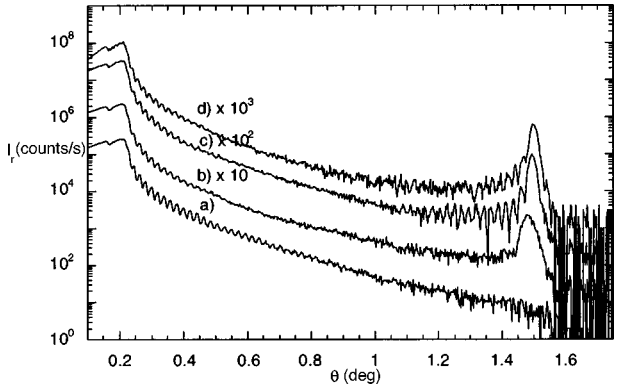

FIG. 5. XRR spectra of a 210-nm thick film annealed at 140 °C for 0 (a), 20 (b), and 120 s (c), and of a film annealed at 160 °C for 20 s (d). The data have been offset for clarity.

sharp edges but very smooth perimeters [Figs. 2(b), 2(c) and 3], which is indicative of a tendency to minimize the length of circumference, i.e., a line tension operates. The time scale in which this layering process takes place is another striking point; it all happens (for these temperatures) within a few minutes.

In the following, we try to interpret these results. Clearly, a description in terms of equilibrium does not make sense, since this would always require the total free energy and, hence the total surface area to be minimal. Hence, we have to consider the sample history. This brings us to the following scenario.

Below the isotropization temperature (T_i) the amorphous phase is metastable. As soon as the initially vitreous polymer is heated to a temperature above T_g in the smectic range, liquid crystalline (LC) domains may nucleate anywhere in the film. These nuclei are oriented randomly. As they grow, they will eventually reach the surface of the film, but this does not stop their growth. Should the crystallization go on, this would eventually lead to a polycrystalline material with a concomitant rough surface. However, this is not the only process. Simultaneously with the crystallization in the bulk of the film, a macroscopic crystal begins to grow from the surface of the substrate upward. The presence of such a crystal could be demonstrated with x-ray reflectivity. An extensive description of the x-ray data is given in Sec. III B. However, in Fig. 4 we already present an electron-density profile (as extracted from a model fit of the x-ray reflection spectrum [4]) for a film of 210-nm thickness, which was annealed during 20 s at 140 °C. After such a short time the topography of the free surface of this polymer film (as monitored by AFM) does not show any terraces yet [surface topography comparable with the one given in Fig. 2(a)]. Still, we find that about 45 ordered layers are present at the substrate surface, whereas the top layer is not yet stratified in this way. This proves that a large crystal is growing from the wafer in the direction of the polymer-air interface. It seems that the substrate acts as an external field in imposing the orientation. This is not very surprising, because we expect attractions between the maleic anhydride groups in the polymer backbone and the silicon surface [15–18], which will help to impose the ordering. Some ordering is even present above the isotropization temperature in the form of a single stable bilayer as shown in a previous work [9]. Obviously, the *free* surface does not act like an external field (in contrast to the case of lamellar ordering in thin copolymer films [19,20]) and this surface then becomes rough. Somewhat later, the terraces appear. Apparently, the large stable crystal grows at the expense of the smaller domains that were responsible for the roughness. It is this Ostwald ripening process, or recrystallization that produces the layering, while preserving the corrugations formed in the first few seconds, with terraces as a result. Apparently, molecules are not transported over large distances, so that macroscopic smoothing cannot occur, or occurs very slowly.

Somewhat similar ''landscapes'' have been observed during deposition of thin silver films [21]. However, the mechanism of formation is different: the Ag terraces are a consequence of layer-by-layer growth of an Ag(111) crystal from the vapor phase, induced by the presence of surface active additives like Sb. Hence, new material is *added* in the course of time, in contrast to what occurs in our system where there is *no* transport from a dilute phase.

B. Kinetics of one-dimensional (re)crystallization

The growth of the layered structures in time in films of about a 200-nm thickness was examined more closely by XRR. With this technique it is possible to follow the layering process in the direction perpendicular to the substrate surface. The samples were annealed at different temperatures in the mesophase at 105, 115, 140, 147, 155, 160, and 164 °C, respectively. The as-prepared films show Kiessig fringes in the reflectograms (an example is given in Fig. 5, trace a), which indicates that the surfaces are smooth.

Upon annealing these fringes remain, but also a Bragg peak appears at a certain moment in the reflectivity curves at all temperatures mentioned above. In Fig. 5 examples are given for films annealed at 140 and 160 °C, respectively.

The Bragg reflectivity arises from the periodicity of the layers. Its intensity increases with annealing time, which reflects the increase in the number of ordered layers in time. The Bragg peak occurs around $\theta = 1.5°$. From Fig. 5 it is clear that in the course of time the position of the peak shifts to higher angles, from about 1.45 to 1.5°. This corresponds to a (small) decrease in layer spacing from 3.0 to 2.9 nm. Furthermore, upon reaching the final stage of layering the Bragg peak becomes narrower and additional Kiessig fringes

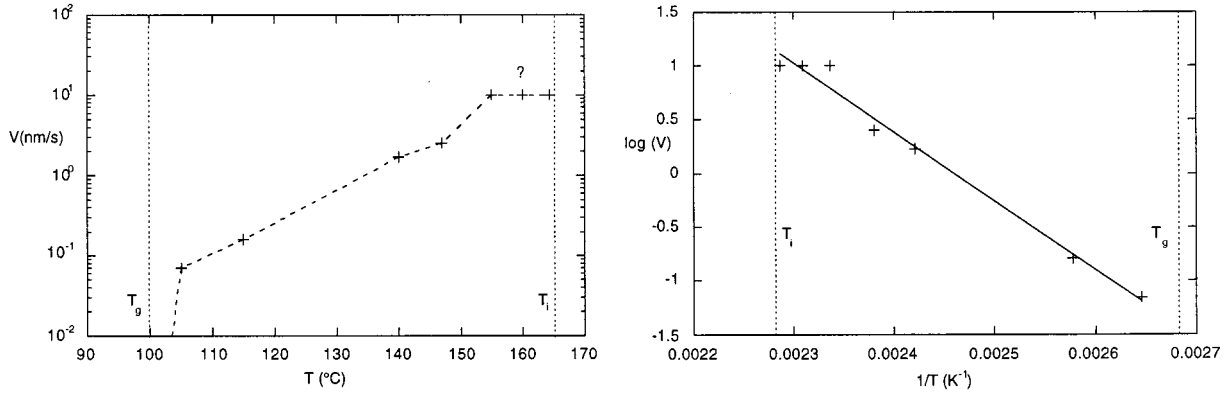

FIG. 6. (a) One-dimensional crystal growth rate at different temperatures and (b) Arrhenius plot of (a). The base of the logarithm is 10.

appear around the Bragg peak. The observations mentioned above (intensity increase, sharpening, and structuring of the peak) indicate that the system becomes more and more ordered. Finally, a perfect one-dimensional crystal appears.

The time after which the Bragg reflections appear depends on the annealing temperature. At 105 °C, just above the T_g, the Bragg peak is hardly visible even after annealing for 7 min (not shown). At higher annealing temperatures the Bragg peak appears sooner and its intensity increases faster. When annealed just below T_i, the Bragg peak has already reached its maximum intensity and established its detailed surrounding fringe structure within the first annealing treatment of 20 s (Fig. 5). A further annealing step has hardly any further effect on the reflectivity curves. This was even the case at temperatures very close to T_i, i.e., nearly 164 °C!

From the reflectivity spectra it is possible to extract the number of ordered layers by using model-fit calculations. In the model we make use of the fact that we have a stack of interdigitated bilayers, each of which can be separated into four regions. As reported in another paper [4] the different regions within one bilayer are successively a backbone region, a spacer region, a mesogenic region, and another spacer region. Important parameters in the model are film thickness, interfacial roughness, electron density per region, number of bilayers, and (sometimes) fluctuations or a gradient in the bilayer spacing.

The number of bilayers was determined after successive annealing steps. Because of the fluctuations in the ordering it was sometimes not possible to do this with high precision. The overall accuracy is about 5–10%. From the number of layers found at different annealing times and temperatures the rate of monocrystal growth (nm/s) can be determined. This rate is plotted in Fig. 6(a) as a function of temperature. As was stated above, the crystal layer growth depends strongly on the temperature. In the case of annealing above 155 °C layering was already complete in less than 20 s of annealing, corresponding to a growth rate of at least 10 nm/s. Since our sample preparation (annealing) procedure does not allow us to determine the actual rate in this case, a question mark is shown in Fig. 6(a).

As mentioned in the Introduction, the viscosity and the undercooling together determine the rate of crystal growth of common (polymer) crystals. However, in our case we are dealing with a kind of recrystallization. The driving force is then not the free-energy difference at the phase boundary (which is proportional to the undercooling for common crystal growth) but it is the reduction of the domain surface energy [22]. Indeed, in our case, it seems that undercooling plays no (or only a very minor) role, since even at less than 1 degree below the isotropization temperature, i.e., hardly any undercooling, the layering occurs very fast.

An important aspect of the recrystallization process is the difference in orientation between the large crystal that starts from the substrate surface and the polycrystalline domains. Since this difference determines domain boundaries, reorientation of only the mesogenic groups at the grain boundary is enough to produce growth of the large single crystal; transport over large distances is not necessary. The viscosity plays the major part in these reorientations, hence also in our ordering process.

When the material is less viscous it is easier for the mesogenic groups to rotate around the backbone. In terms of dielectric spectroscopy this rotational motion gives rise to the so-called δ relaxation, which has been studied for different side-chain liquid-crystalline polymers (spacer length about 5–8 carbon atoms) [23–26]. In those studies this reorientation process was investigated as a function of the temperature, showing an Arrhenius-type temperature dependence from which the activation energy E_{act} can be derived. Typical values found are around 150–180 kJ/mol. In the case of small nematogens, i.e., low molecular weight liquid crystals, activation energies in the range of 60–90 kJ/mol have been reported [27]. In the former case, the rotation is evidently more cooperative and micro-Brownian motions of the polymer are a necessary prerequisite.

When we make an Arrhenius plot of our data [Fig. 6(b)] we also obtain a straight line. The activation energy, derived from the slope according to the Arrhenius equation $\ln V = -E_{\mathrm{act}}/RT + \mathrm{const}$, gives $E_{\mathrm{act}} = 122$ kJ/mol. This value is in between the values obtained from dielectric measurements for other LCP and LC systems, as discussed above. Since our polymers are very short ($n = 10$) and are actually oligomers, it is plausible that the motion of the mesogenic groups is less restricted by the motion of the backbone than for polymers of high molar mass ($n \cong 50$). Compared to small nematogens, of course, the motion will be more restricted. Hence, one may anticipate an intermediate activation energy, in between that for LCPs and for LCs, as indeed found for our system.

IV. CONCLUSIONS

Initially rough films of an isotropic polymer normally tend to become smooth upon heating in order to lower the surface free energy. However, films of a thermotropic side-chain liquid-crystalline polymer can be highly anisotropic and behave quite differently. Initially, the crystallization process in the film occurs in randomly oriented domains. However, at the substrate surface a large crystal of parallel-ordered (bi)layers starts to grow from the surface. This laterally macroscopic crystal grows at the expense of the randomly oriented domain structures until the whole film is layered parallel to the substrate surface. The crystal growth rate depends strongly on the temperature and increases by more than two orders of magnitude over the whole mesophasic temperature range. In this crystallization process the effect of polymer viscosity dominates; the effect of undercooling is very small since our films undergo a *re*crystallization process. Rotation of the mesogenic groups around the polymer backbone is enough to promote layer growth in the film. The activation energy for this process is 122 kJ/mol, as derived from an Arrhenius plot. This value is in the expected range, taking data for other systems (LCP and LC) obtained by dielectric spectroscopy into account.

At the end of the recrystallization process a super crystal remains with very striking nanosized surface patterns. This ''molecular landscaping'' process may have interesting applications if it can be externally controlled. It is clear from our result that the growth of the macroscopic crystal retains, to some extent, the initial surface topography. We, therefore, could speculate that it would be possible to mechanically impose a certain surface topography, which subsequently could be annealed towards a perfectly terraced surface structure.

ACKNOWLEDGMENTS

We thank A. J. G. Leenaers (Philips Research Laboratories, Eindhoven) for participating in the x-ray reflectivity measurements and R. P. Nieuwhof (Wageningen University) for providing the liquid-crystalline polymer. This work was supported by the Dutch Ministry of Economic Affairs through the SENTER ''IOP-verf'' program.

[1] H. Mensinger, M. Stamm, and C. Boeffel, J. Chem. Phys. **96**, 3183 (1992).
[2] H. Elben and G. Strobl, Macromolecules **26**, 1013 (1993).
[3] G. Henn, M. Stamm, H. Poths, M. Rücker, and J. P. Rabe, Physica B **221**, 174 (1996).
[4] M. W. J. van der Wielen, M. A. Cohen Stuart, G. J. Fleer, D. K. G. de Boer, A. J. G. Leenaers, R. P. Nieuwhof, A. T. M. Marcelis, and E. J. R. Sudhölter, Langmuir **13**, 4762 (1997).
[5] G. Reiter, and J.-U. Sommer, Phys. Rev. Lett. **80**, 3771 (1998).
[6] K. Izumi, G. Ping, M. Hashimoto, A. Toda, H. Miyaji, Y. Miyamoto, and Y. Nakagawa, *Advances in the Understanding of Crystal Growth Mechanisms* (Elsevier Science, B.V., 1997), p. 337.
[7] F. A. Bovey and F. H. Winslow, *Macromolecules* (Academic, New York, 1979).
[8] H.-G. Elias, *Macromolecules 1* (Plenum, New York, 1983).
[9] M. W. J. van der Wielen, M. A. Cohen Stuart, and G. J. Fleer, Langmuir **14**, 7065 (1998).
[10] R. P. Nieuwhof, A. T. M. Marcelis, E. J. R. Sudhölter, M. W. J. van der Wielen, M. A. Cohen Stuart, and G. J. Fleer, Macromol. Symp. **127**, 115 (1998).
[11] R. P. Nieuwhof, A. T. M. Marcelis, E. J. R. Sudhölter, E. J. R. Picken, and W. H. de Jeu, Macromolecules **32**, 91 (1999).
[12] D. K. G. de Boer, A. J. G. Leenaers, and W. W. van der Hoogenhof, X-Ray Spectrom. **24**, 91 (1995).
[13] A. J. G. Leenaers, and D. K. G. de Boer, X-Ray Spectrom. **26**, 115 (1997).
[14] D. Ausserré, F. Brochard-Wyart, and P.-G. de Gennes, C. R. Acad. Sci., Ser. IIb: Mec., Phys., Chim., Astron. **320**, 131 (1995).
[15] W. Funke, Prog. Org. Coat. **28**, 3 (1996).
[16] J. Gähde, R. Mix, R.-P. Krüger, and H. Goering, J. Adhes. **58**, 243 (1996).
[17] J. Gähde, R. Mix, H. Goering, G. Schulz, W. Funke, and U. Hermann, J. Adhes. Sci. Technol. **11**, 861 (1997).
[18] R. A. Kurbanova, R. Mirzaoglu, S. Kurbanov, I. Karatas, V. Pamuk, E. Ozcan, A. Okudan, and E. Güler, J. Adhes. Sci. Technol. **11**, 105 (1997).
[19] T. P. Russell, G. Coulon, and D. C. Miller, Macromolecules **22**, 4600 (1989).
[20] A. M. Mayes, T. P. Russell, P. Bassereau, P. Bassereau, S. M. Baker, and G. S. Smith, Macromolecules **27**, 749 (1994).
[21] J. Vrijmoeth, H. A. van der Vegt, J. A. Meyer, E. Vlieg, and R. J. Behm, Phys. Rev. Lett. **72**, 3843 (1994).
[22] R. H. Doremus, *Rates of Phase Transformations* (Academic, New York, 1985).
[23] J. H. Wendorff and T. Fuhrmann, *Dielectrics Newsletter* (Novocontrol GmbH, Hundsangen, 1994), p. 1.
[24] G. S. Attard, G. Williams, G. W. Gray, D. Lacey, and P. A. Gemmel, Polymer **27**, 185 (1986).
[25] W. Heinrich and B. Stoll, Colloid Polym. Sci. **263**, 895 (1985).
[26] R. Zentel, G. R. Strobl, and H. Ringsdorf, Macromolecules **18**, 960 (1985).
[27] M. Davies, R. Moutran, A. H. Price, M. Beevers, and G. Williams, J. Chem. Soc., Faraday Trans. 2 **72**, 1447 (1976).